Original Article
Food Science and Technology

ISSN 0101-2061 (Print)
ISSN 1678-457X (Online)

DOI: https://doi.org/10.1590/fst.122821

Effects of quercetin on renal autophagy and interstitial fibrosis in diabetes mellitus

Shuling WANG[1], Sainan SHANG[1], Juan LV[1], Dandan HOU[1]*

Abstract

To observe the effect of quercetin (Que) on renal autophagy level and renal interstitial fibrosis in the mice with diabetes mellitus (DM),and to discuss the possible mechanism. The wild-type C57BL/6 mice were randomly divided into 3 groups,including normal control (Normal) group, DM group and Que group (n = 9 in every groups). The diabetic mouse model was established by injection of streptozotocin. After 8 weeks of successful replication of the diabetic model,Que was given to the mice in Que group by continuous gavage for 12 weeks,and then the mice in each group were sacrificed to detect the relevant biochemical parameters. The pathological changes of the kidney tissues were observed by HE staining and Masson staining. The levels of the proteins related to autophagy,epithelial-mesenchymal transition(EMT)and fibrosis were determined by Western blot. The mRNA expression of collagen type IV (Col IV),α-smooth muscle actin(α-SMA)and E-cadherin were detected by real-time PCR. Compared with Normal group, fasting blood glucose (FBG), kidney index (KI),serum creatinine, 24-hour urinary albumin excretion rate and 24-hour urine total protein were remarkably increased in DM group ($P < 0.001$). The results of HE and Masson staining indicated that renal tissue presented fibrosis in DM group. The protein levels of E-cadherin,beclin-1,microtubule-associated protein 1 light chain 3-II (LC3-II)/LC 3I ratio were reduced in DM group,while the levels of α-SMA,Col IV and Snail1 were increased ($P < 0.001$). After intervention with Que for 12 weeks,all the relevant biochemical parameters and KI were reduced ($P < 0.001$) except FBG ($P > 0.05$), and renal fibrosis lesions were obviously alleviated. Compared with DM group,the protein levels of E-cadherin,beclin-1 and LC3-II were increased in Res group,but the protein expression levels of α-SMA,Col IV,Snail1 were reduced($P < 0.001$). Compared with DM group, the mRNA level of E-cadherin was increased in Que group, but the mRNA levels of Col IV and α-SMA were reduced ($P < 0.001$). Quercetin significantly inhibits EMT and reduces renal interstitial fibrosis in diabetic mice,and its mechanism may be related to the promotion of renal autophagy.

Keywords: quercetin; renal interstitial fibrosis; endothelial-mesenchymal transition; autophagy.

Practical Application: Quercetin improved renal autophagy and interstitial fibrosis in diabetes mellitus.

1 Introduction

Diabetes mellitus (DM) is a chronic endocrine disorder with a sustained incidence currently in the world. While diabetic nephropathy (DN) is a common microvascular complication of DM, which is also considered as one of the main causes leading to end-stage renal disease (ESRD) and death (Luis-Rodríguez et al., 2012). Tubulointerstitial fibrosis is one of the main pathological changes from DN to ESRD. During the process, the epithelial-mesenchymal transition (EMT) in renal tubular epithelial cells functions significantly in promoting renal interstitial fibrosis (Loeffler & Wolf, 2015). However, it is still unclear with respect to the specific mechanism so far. Furthermore, autophagy is a conserved mechanism for protein degradation. Through the mediation by the lysosomal pathway, aging proteins and damaged organelles can be removed intracellularly, which is of great significance to maintaining their own homeostasis and cell integrity. It has been reported that the level of autophagy was significantly inhibited in the renal tissue of DN rats (Koch et al., 2020). Significantly, increasing the level of autophagy has been demonstrated to significantly inhibit the occurrence and development of renal fibrosis and DN (Ma et al., 2016). All the above evidence suggests an intimate association of autophagy with the occurrence and development of DN (Wu et al., 2015).

Quercetin (Que) is a natural flavonoid, which is generally present in flowers, leaves and fruits of plants. Que has been discovered in over 100 types of Chinese herbal medicines, vegetables and fruits (Wong et al., 2020). According to previous studies, Que can play a protective role in the kidney by reducing blood glucose, preventing oxidative stress and inflammation, and inhibiting renal fibrosis (Tang et al., 2019; Lin et al., 2020; Liu et al., 2019). Furthermore, Knekt et al. (2002) found in their research that the consumption of Que could reduce the risk of multiple chronic diseases including diabetes. Simultaneously, Castilla et al. (2006) have verified the antioxidant, hypolipidemic and anti-inflammatory effects of Que in hemodialysis patients and healthy subjects. In addition, through a double-blind cross-control experiment in 93 overweight patients in Germany, Egert et al. (2009) proved that Que can reduce systolic blood pressure and low-density lipoprotein concentration. However, it remains unclear with respect to the mechanism of Que in renal interstitial fibrosis. Accordingly, the present study was conducted to observe the effects of Que intervention on renal fibrosis and autophagy in DM mice on the basis of constructing a type 1 DM mouse model using streptozotocin (STZ). It is expected to further explore the effect of Que on renal interstitial fibrosis in DN and to clarify its possible mechanism.

Received 21 Nov., 2021
Accepted 31 Dec., 2021
[1]*Shuangqiao Hospital, Beijing, China*
*Corresponding author: houdandan0511@tom.com

2 Materials and methods

2.1 Animals

Twenty-seven healthy and clean male 6-week-old C57BL/6 mice, weighing (20 ± 5)g, were purchased from SBF (Beijing) Biotechnology Co., Ltd. (license key: SCXK (Beijing) 2016-0002). The experimental animals were normally raised in a constant temperature (25 °C) facility, giving a cycle of 12 hours light and 12 hours dark artificially, and were provided with standard clean-grade feed for 1 week of adaptive feeding.

STZ (Sigma); Que (purity > 98%; Sigma) prepared into suspension with 0.5% sodium carboxymethylcellulose for subsequent use; anti-GAPDH antibody (PuMei Biology); anti-α-SMA and anti-E-cadherin antibodies (Abcam); anti-type IV collagen (Col IV) antibody (Sigma); anti-microtubule associated protein 1 light chain 3(LC3) and anti-Snail1 antibodies (Cell Signaling Technology); anti-beclin-1 antibody (Proteintech); Horseradish peroxidase-labeled sheep anti-rabbit and sheep anti-mouse IgG (Boster); ECL chemiluminescence kit and BCA protein concentration assay kit (Beyotime Biological Research Institute); polyvinylidene fluoride (PVDF) membrane and Whatman 3 MM filter paper (Millipore); RevertAidTM First Strand cDNA Synthesis Kit (Thermo); TB Green Premix Ex TaqTM II (TaKaRa); tissue grinder (Scientz); H-7500 transmission electron microscope (HITACHI, Japan); AU680 automatic biochemical analyzer (Beckman Coulter); Scope A1 straightforward microscope(Zeiss); gel imaging system and fluorescence quantitative PCR instrument (Bio-Rad).

2.2 Main methods

After adaptive feeding for 1 week, the 27 mice were randomly divided into normal control (Normal) group, DM group and Que group, with 9 mice in each group. Mice in the DM group and Que group were weighed before modeling, fasted for 6 hours, anesthetized with ether, and intraperitoneally injected with STZ (55 mg/kg·d) dissolved in sterile citric acid/sodium citrate buffer (pH 4.5, 0.01 mol/L) for 5 days to establish DM mouse model. Mice in the Normal group were given an intraperitoneal injection of an equal volume of STZ with sodium citrate buffer as the solvent. Fasting blood glucose (FBG) was measured by tail vein blood sampling. The model was successfully established when FBG ≥ 16.7 mmol/L and stable for 1 week. After 8 weeks of modeling, mice in the Que group were intervened with Que at the dosage of 10 mg/kg·d for gavage (once a day) by gavage, with Que dissolved in 0.5% sodium carboxymethyl cellulose for fresh preparation. While mice in the DM group and Normal group were given an equal volume of 0.5% carboxymethyl cellulose sodium by gavage once a day. All mice were killed after 12 weeks of continuous administration. During modeling, all mice were fed with standard feed and provided with free access to drinking. Blood glucose and body weight were monitored once a week.

2.3 Blood, urine and renal tissue sampling

One day before the mice were killed, 24 h urine was collected and the urine volume was recorded. After centrifugation, part of the supernatant was taken to detect urinary protein. The mice were fasted for 6 hours before death, anesthetized with ether and weighed, after which the blood was sampled from the orbit, followed by centrifugation at 1 467 × g for 10 min to separate serum for detecting biochemical indexes. After blood collection, the abdominal cavity was cut open to expose bilateral kidneys, the external renal capsule and surrounding adipose tissue were gently removed on ice, with the recording of the weight of bilateral kidneys simultaneously. A part of the tissues was fixed in 4% neutral formaldehyde and prepared into paraffin-embedded sections for pathological examination. The rest of the kidney was cut with the renal medulla removed, which was cryopreserved at - 80 °C for protein extraction and RNA detection to perform Western blot and real-time PCR, respectively. The ratio of kidney weight (mg)/body weight (kg) was calculated as the kidney index (KI).

2.4 Biochemical index detection

FBG was measured by glucose oxidase method, serum creatinine (SCR) by oxidase method, urinary albumin excretion rate (UAER) by immunoturbidimetry, and urinary total protein (UTP) by Pyrogallol red-molybdate complex method. The 24 h UTP and 24 h UAER were calculated by multiplying UTP and UAER by 24 h urine volume, respectively.

2.5 Histological observation of kidney

Part of the renal tissue was fixed in 4% neutral formaldehyde, embedded and fixed, and made into paraffin-embedded sections of 3 μm in thickness, followed by HE and Masson staining after dewaxing. The morphological changes of renal tissue in each group were observed under the common light microscope.

2.6 Observation of the ultra-structure of mouse kidney by transmission electron microscope (TEM)

Renal tissue was fixed with 2.5% glutaraldehyde and then fixed with 1% osmic acid, followed by dehydration, soaking, embedding and slicing. The prepared sections were double-stained with uranium acetate and lead citrate, and the results were observed under the electron microscope.

2.7 Western Blotting (WB) detection of the protein expression levels of fibrosis index, EMT indexes and autophagy-related indexes in renal tissues

An amount of 0.2g renal cortical tissue was weighed into a 1.5 mL autoclaved EP tube, with the addition of 1mL tissue protein lysate (RIPA: PMSF = 97:3), and placement of magnetic beads into the tube, which was fully ground into liquid by tissue grinder. The supernatant was collected after centrifugation at 4 °C and 13,201 × g. After protein quantification by the BCA method, an appropriate amount of loading buffer was added based on the concentration, which was heated in boiling water at 100 °C for 10 min after fully mixing. With sample loading, the protein was separated by SDS-PAGE, followed by membrane transfer at 300 mA to PVDF membrane, and sealing with 5% skimmed milk at room temperature for 1 h, After TBST washing (10 min, 3 times), the primary antibodies [GAPDH (1: 4 000), LC3 (1: 1 000), Beclin--1 (1: 1 000), Col IV (1: 500), α-SMA (1: 1 000), E-cadherin (1: 1 000) and Snail1 (1: 1 000)] were added for overnight incubation at 4 °C. With the recovery of the primary

antibodies the next day, the corresponding horseradish peroxidase-labeled secondary antibody was added for 1 h of incubation at room temperature after membrane washing using TBST. With another membrane washing, ECL developer (1:1) was added and mixed well in dark. The Bio-Rad gel imager was used for visualization, and Image Lab 5.1 software was used to scan protein bands and analyze the gray value. The protein expressions of the target proteins were normalized to GAPDH relative expression.

2.8 Real-time PCR detection of α-SMA, E-cadherin and Col-IV mRNA expression levels

An amount of 0.1 g of the renal cortex was added with 1 mL of TRIzol to extract RNA from mouse renal tissue. After the concentration and purity of RNA were measured at the wavelength of 260/280 nm by using a nucleic acid spectrometer, the RNA was reverse transcribed into cDNA according to the Thermo kit. After that, PCR reaction was performed according to TaKaRa TB Green Premix Ex TaqTM II kit with 20 μL of the reaction system. The primers of α-SMA, E-cadherin, Col IV and β-actin were designed by using DNAMAN software, which were then synthesized by Sangon Biotech (Shanghai) Co., Ltd. Bio-Rad CFX96™ fluorescence quantitative PCR analysis system was used for detection, and the melting curve analysis was utilized to evaluate the reliability of PCR results. PCR reaction included: at 95 °C for 3 min; at 95 °C for 10 s, at 55 °C for 30 s (39 cycles); and at 72 °C for 10 s. With β-actin as the internal reference, the relative expression of the target genes was expressed as $2^{-\Delta\Delta Ct}$. ΔΔCt = [Ct target gene (test sample)-Ct internal reference gene (test sampled)]- [Ct target gene (calibration sample)-Ct internal reference gene (calibration sample)]. Table 1 shows the sequences of primers.

2.9 Statistical analysis

SPSS 17.0 software was used for analysis. The data were all expressed as mean ± standard deviation (mean ± SD) and were compared by one-way analysis of variance. $P < 0.05$ was considered to have a statistically significant difference.

Table 1. The sequences of the primers used in real-time PCR.

Name	Primer sequence
α-SMA	F:5'-ACACGGCATCATCACCAACT-3'
	R:5'-AGAGGCATAGAGGGACAGCA-3'
Col IV	F:5'-AACAACGTCTGCAACTTCGC-3'
	R:5'-TGACTGTGTACCGCCATCAC-3'
E-cadherin	F:5'-CATCGCCTACACCATCGTCA-3'
	R:5'-CCCTGATACGTGCTTGGGTT-3'
β-actin	F:5'-GTGCTATGTTGCTCTAGACTTCG-3'
	R:5'-ATGCCACAGGATTCCATACC-3'

F: forward; R: Reverse.

3 Results

3.1 Comparison of metabolic and biochemical indexes of mice in each group

As shown in Table 2, FBG, KI, SCr, 24 h UAER and 24 h UTP were all significantly higher in the DM group than those in the Normal group ($P < 0.01$). While compared with the DM group, the Que group showed obviously lower KI, SCr, 24 h UAER and 24 h UTP ($P < 0.01$). But there was no difference in FBG between the DM group and the Que group ($P > 0.05$).

3.2 Pathological changes of renal tissue in each group

According to the results of HE and Masson staining, the Normal group had a clear renal tubular structure, orderly arranged epithelial cells, relatively complete basement membrane, and none obvious interstitial inflammatory cell infiltration and collagen deposition. Compared with the Normal group, the DM group showed congested and dilated glomeruli, vacuolated, necrotic, atrophic and exfoliated renal tubular epithelial cells partially, and infiltrated inflammatory cells around renal tubules and renal interstitium (Figure 1), accompanied by significant deposition of blue-stained collagen fibers. Furthermore, relative to the DM group, there were alleviated renal lesions, mild glomerular congestion, mitigated renal tubulointerstitial fibrosis, and reduced collagen deposition in the Que group. Statistical analysis revealed that the collagen volume fraction of renal tissue was significantly higher in the DM group than that in the Normal group ($P < 0.001$, Figure 2). While following the Que group, the Que group had significantly improved collagen volume fraction of renal tissue when compared with the DM group ($P < 0.001$, Figure 2).

3.3 Ultra-structure of mouse kidney

As presented in Figure 3, in the Normal group, the nuclei were spherical or elliptical with less heterochromatin; The lumen of the endoplasmic reticulum was thin and narrow, showed reticular appearance and connected into pieces; mitochondria were mostly spherical or oval, ridged, and not wrapped by endoplasmic reticulum; lysosomes were few in amount and spherical in shape; besides, there were visible autophagosomes, as well as relatively less and smaller lipid droplets. While in the DM group, nuclear heterochromatin increased and the nucleus was irregular in shape; the lumen of the endoplasmic reticulum

Table 2. The kidney index(KI), fasting blood glucose (FBG), 24-hour urinary albumin excretion rate (24 h UAER), 24-hour urine total protein(24 h UTP) and serum creatinine(SCr) in each group (Mean ± SD. n=9).

Group	KI (%)	FBG (mmol/L)	24 h UAER (mg)	SCr (μmol/L)
Normal	1.28 ± 0.02	10.56 ± 0.27	15.73 ± 0.77	15.72 ± 0.49
DM	1.93 ± 0.03**	23.45 ± 0.30**	313.24 ± 33.40**	41.76 ± 0.44**
Que	1.55 ± 0.07##	23.60 ± 0.39	146.58 ± 15.56##	17.48 ± 0.85##

**: $P < 0.01$, compared with Normal. ##: $P < 0.01$, compared with DM group.

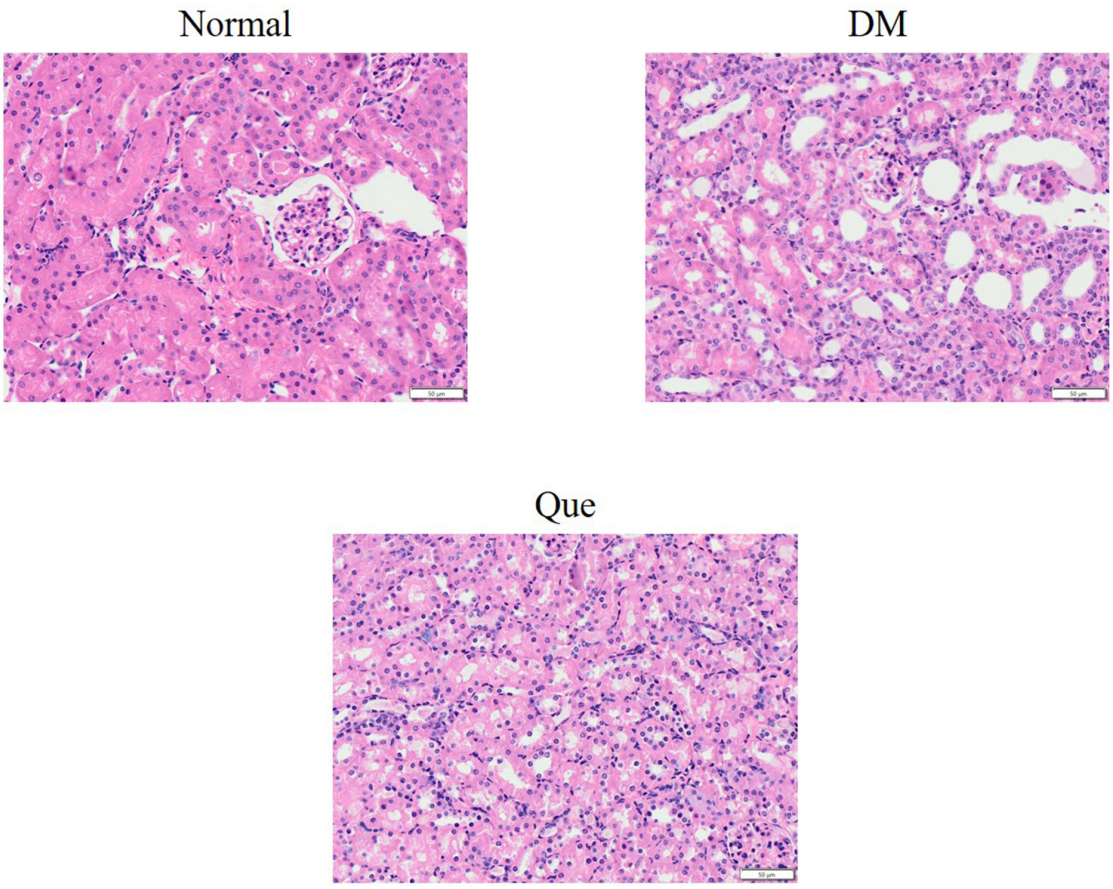

Figure 1. The histological change by HE staining (×200). Normal: The normal control mice; DM: The DM model mice; Que: The DM model mice were treated with Que.

expanded, with a tendency to wrap mitochondria and disordered distribution; mitochondria were mostly irregular, with swelling or shrinking, or stretching and growing with curved strips, with a trend of cyclization; and there were fewer autophagosomes. In addition, in the Que group, the endoplasmic reticulum tended to wrap mitochondria and distributed disorderly; mitochondria were irregular and damaged in appearance; there are large lipid droplets and more autophagosomes.

3.4 Protein expression levels of fibrosis index (Col IV) and EMT indexes (α-SMA, E-cadherin and Snail1) in renal tissues of each group

DM group showed significant upregulation in the protein expressions of Col IV, α-SMA and Snail1 in renal tissues than those in the Normal group, and obviously downregulation in E-cadherin protein expression than that in the Normal group ($P < 0.001$, respectively, Figure 4). While compared with the DM group, the Que group had remarkably downregulated Col IV, α-SMA and Snail1 protein expressions, and highly upregulated E-cadherin protein expression ($P < 0.001$, Figure 4). Furthermore, the DM group revealed much higher mRNA expressions of Col IV and α-SMA in renal tissues, and much lower E-cadherin mRNA expression ($P < 0.001$, respectively, Figure 5). Meanwhile, relative to the DM group, there was increased E-cadherin mRNA expression ($P < 0.001$, respectively, Figure 5), but decreased Col IV and α-SMA mRNA expressions in the Que group ($P < 0.001$, respectively, Figure 5).

3.5 Protein expression levels of autophagy-related indexes (Beclin-1 and LC3) in renal tissues of each group

Compared with Normal, group, the DM group showed downregulated autophagy-related index Beclin-1 protein expression, and decreased ratio of LC3-II/LC3-I ($P < 0.001$, Figure 6). Besides, there were significantly increased protein expression of Beclin-1 and elevated ratio of LC3-II/LC3-I in the Que group than those in the DM group ($P < 0.001$, Figure 6).

4 Discussion

DN has been considered as one of the main causes of ESRD [1], and its pathological changes include glomerulosclerosis and renal interstitial fibrosis. While renal interstitial fibrosis is generally manifested as the injury of renal tubular epithelial cells and the accumulation of massive extracellular matrix (ECM). As evidenced by prior researches, EMT of renal tubular epithelial cells is critical in promoting the deposition of ECM, renal interstitial fibrosis as well as the occurrence and development

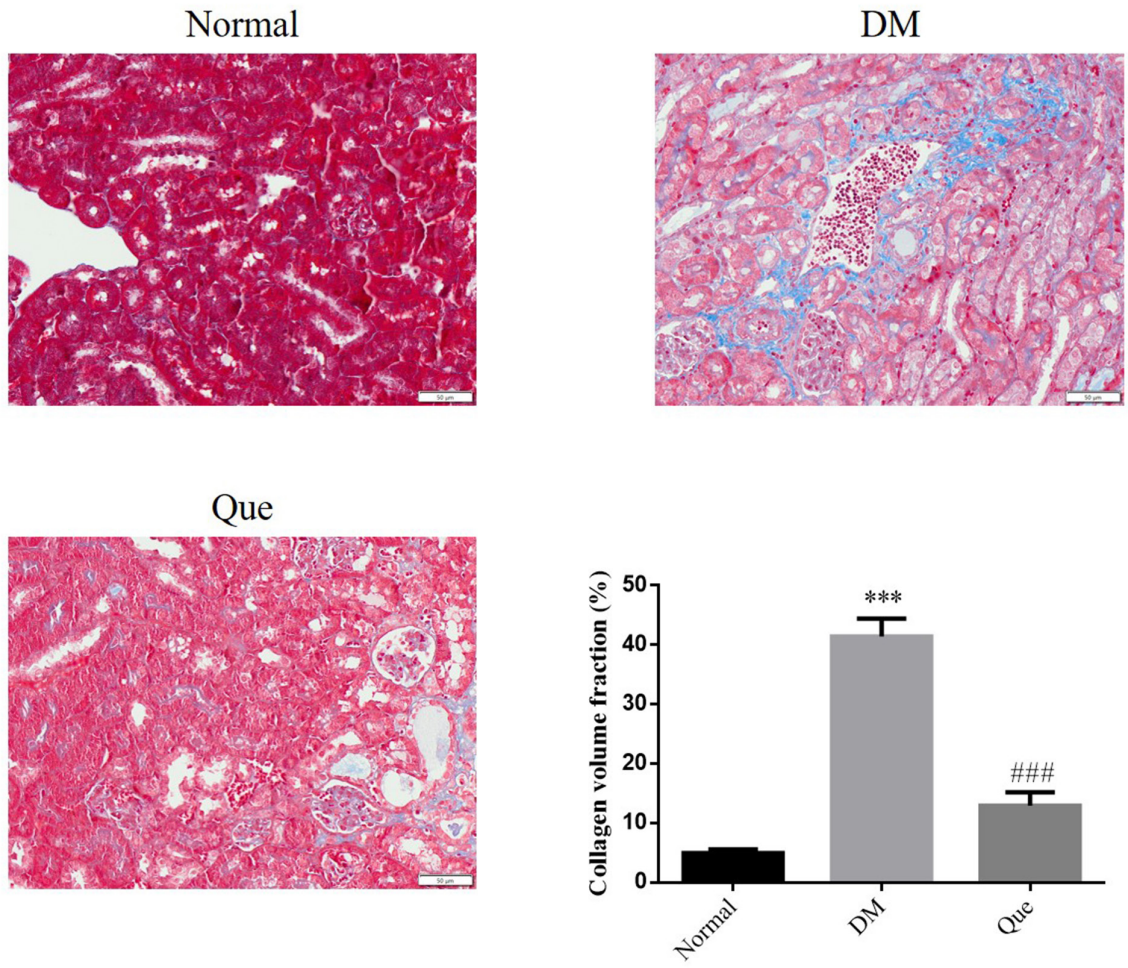

Figure 2. The histological change by Masson staining (×200). Normal: The normal control mice; DM: The DM model mice; Que: The DM model mice were treated with Que.***: P < 0.001, vs. Normal group; ###: P < 0.001, vs. DM group

of DN (Loeffler & Wolf, 2015; Xu et al., 2020). Among them, as the initiator of EMT, transcription inhibitor Snail1 may be crucial in the process (Recouvreux et al., 2020). Snail1 can inhibit the expression of E-cadherin by binding to the E-box of the E-cadherin promoter region, and can also induce the expression of α-SMA. For instance, in high glucose cultured renal tubular epithelial cells, the occurrence of EMT can be promoted by promoting the expression of Snail1, which, however, could be inhibited by inhibiting its expression (Bai et al., 2016; Lu et al., 2015). In our experiment, the animal model of interstitial fibrosis of DN was constructed successfully, as evidenced by the biochemical indexes and pathological changes of the DM group. Moreover, compared with the Normal group, the DM group showed increased expressions of α-SMA, Col IV and Snail1, but reduced expression of E-cadherin (P < 0.001, respectively), suggesting the occurrence of fibrosis and EMT in this process.

Autophagy is one of the two pathways of lysosome-dependent protein degradation intracellularly (Vindis, 2015). It plays an important role in many physiological and pathological conditions, such as metabolism, degenerative and malignant diseases, etc. (Kim & Lee, 2014; Rohatgi & Shaw, 2016). For example, Huang et al. (2017) detected a significantly inhibited level of autophagy in the renal tissue of db/db mice; and Beclin-1, a key regulator of autophagy formation, was also reported to be obviously decreased in DN rats and high glucose cultured renal tubular epithelial cells, accompanied by the decreased autophagy level (Wu et al., 2015; Xu et al., 2015). In our study, along with the progression of fibrosis, the protein expressions of Beclin-1 and LC3-II in renal tissue of the DM group were evidently lower than those of the Normal group, showing a weakened level of autophagy. These results may indicate that autophagy deficiency may be involved in the occurrence and development of renal fibrosis in DM, and the upregulation of autophagy may be a potential target for DN therapy (Wu et al., 2015). Simultaneously, an elevation in Beclin-1 expression may also contribute to the upregulation of autophagy level and inhibit the occurrence of EMT (Li et al., 2016). According to additional results of our experiment, relative to the Normal group, there existed reduced autophagy corpuscles and Beclin-1 expression, significantly increased expression of Snail1, and obvious fibrosis in renal tissue of DM group, suggesting that autophagy regulated by Beclin-1 has an intimate association with EMT. Furthermore, after intervention with Que, DM mice

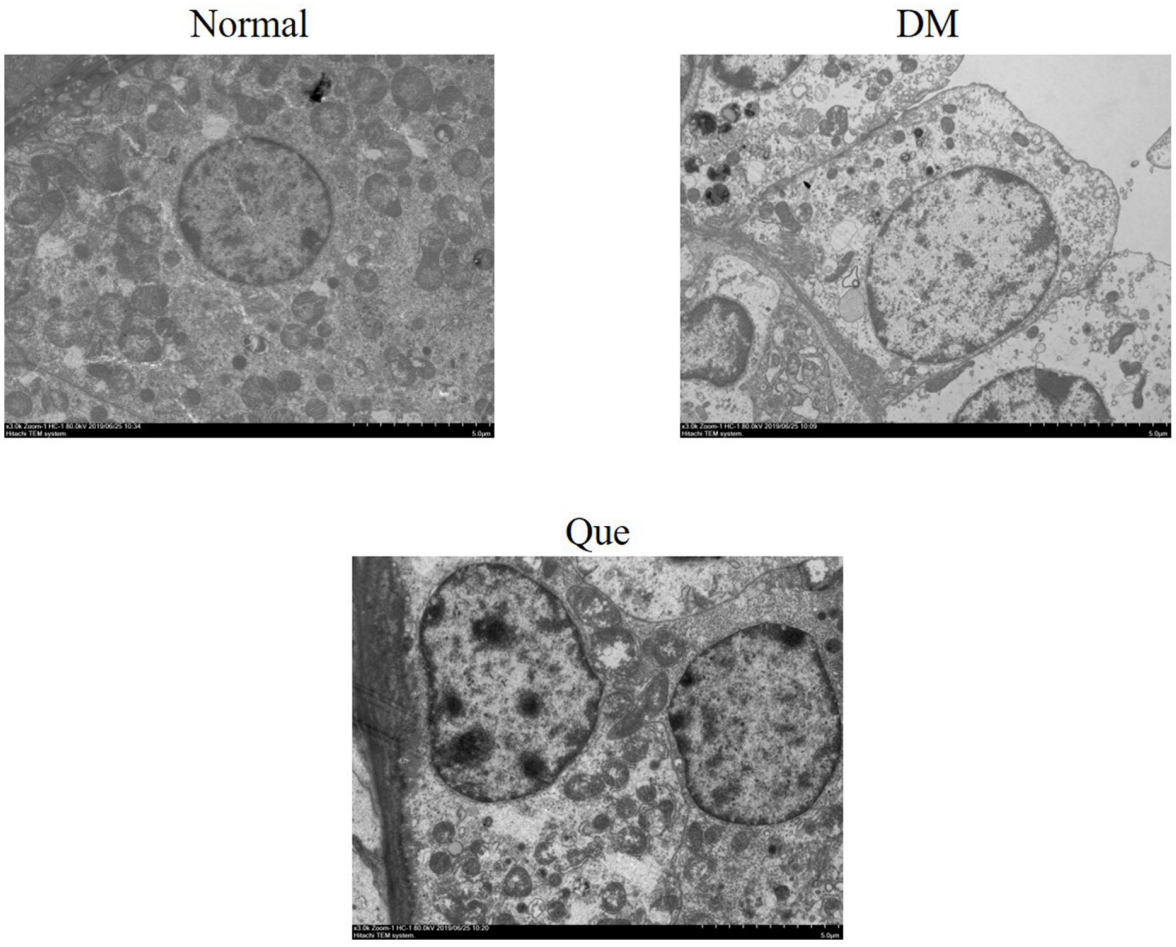

Figure 3. Transmission electron microscope observation kidney tissues.Normal: The normal control mice; DM: The DM model mice; Que: The DM model mice were treated with Que.

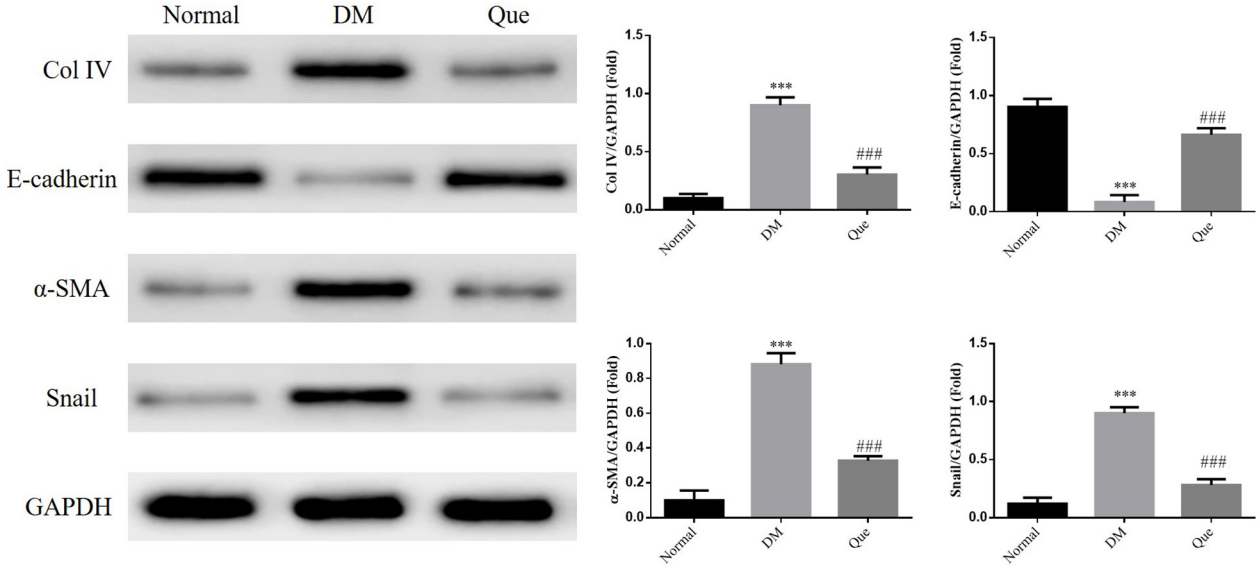

Figure 4. Col IV, E-cadherin, α-SMA and Snail protein expression by WB assay. Normal: The normal control mice; DM: The DM model mice; Que: The DM model mice were treated with Que.***: $P < 0.001$, vs. Normal group; ###: $P < 0.001$, vs. DM group.

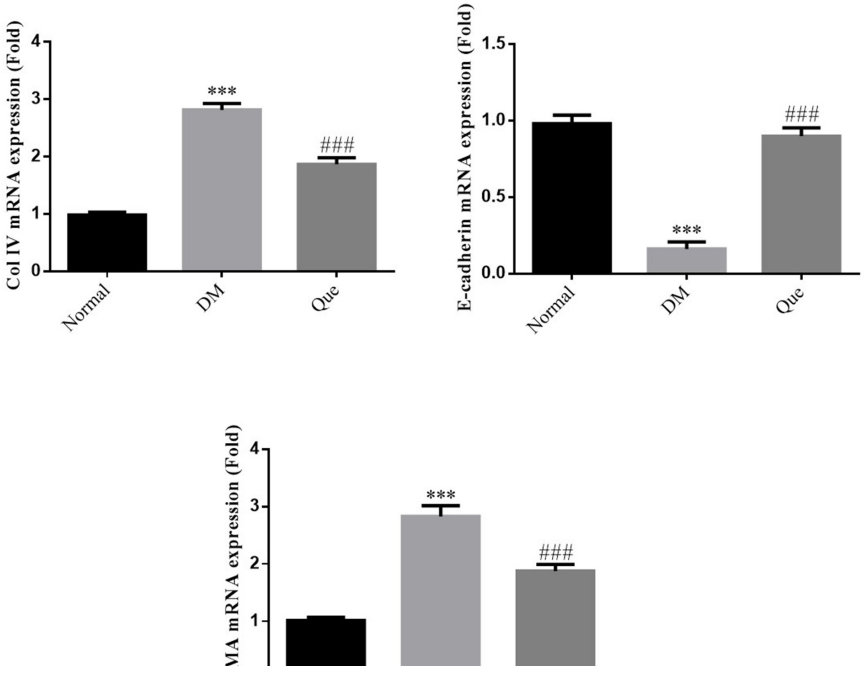

Figure 5. Col IV, E-cadherin, α-SMA and Snail mRNA expression by WB assay. Normal: The normal control mice; DM: The DM model mice; Que: The DM model mice were treated with Que.***: P < 0.001, vs. Normal group; ###: P < 0.001, vs. DM group.

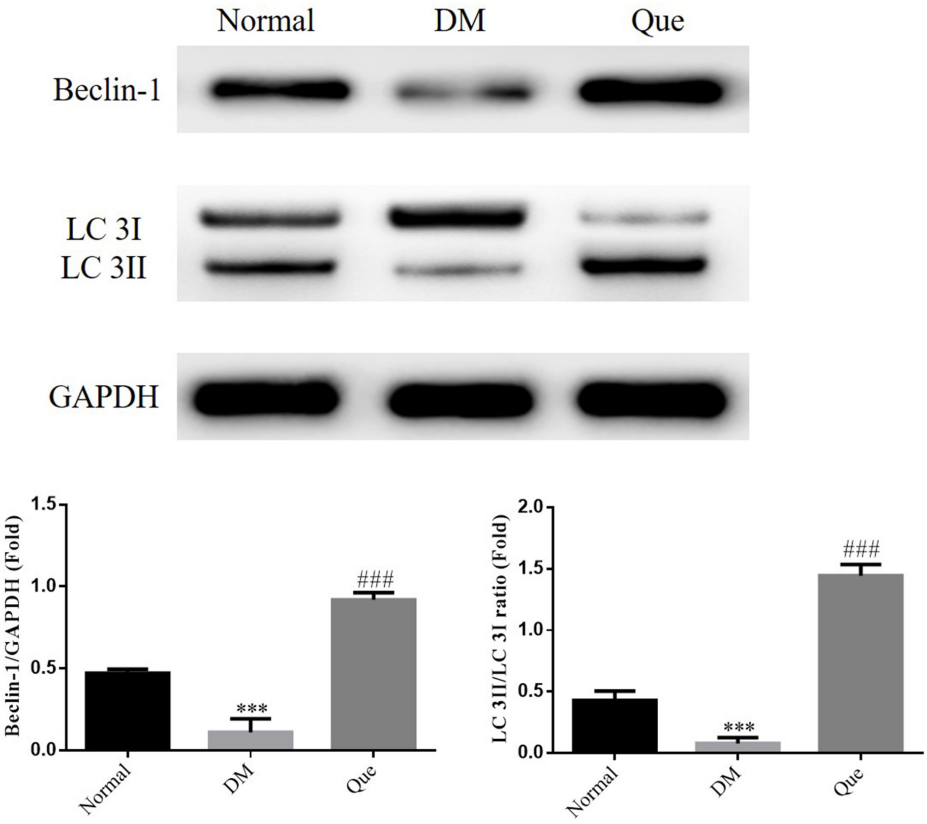

Figure 6. Beclin-1 and LC 3 protein expression by WB assay. Normal: The normal control mice; DM: The DM model mice; Que: The DM model mice were treated with Que. ***: P < 0.001, vs. Normal group; ###: P < 0.001, vs. DM group.

showed upregulated level of autophagy and obviously reduced degree of fibrosis. Compared with the DM group, the Que group revealed remarkably increased autophagosomes, obviously upregulated Beclin-1 expression, decreased Snail1 expression, as well as alleviated fibrosis and EMT in the renal tissue of mice. Collectively, Que may protect the kidney from injury by promoting Beclin-1 expression, upregulating autophagy level, enhancing Snail1 degradation, reliving renal fibrosis and inhibiting the occurrence and development of renal interstitial fibrosis and EMT in DM mice.

In conclusion, Que has a protective role in DN, and its mechanism may be related to the upregulation of autophagy level mediated by Beclin-1 and downregulation of Snail1 expression, so as to delay renal fibrosis and protect the kidney. While it still remains to be clarified and deserves to be explored with respect to the specific relationship between Beclin-1 and Snail1 in DN.

References

Bai, X., Geng, J., Zhou, Z., Tian, J., & Li, X. (2016). MicroRNA-130b improves renal tubulointerstitial fibrosis via repression of snail-induced epithelial-mesenchymal transition in diabetic nephropathy. *Scientific Reports*, 6(1), 20475. http://dx.doi.org/10.1038/srep20475. PMid:26837280.

Castilla, P., Echarri, R., Dávalos, A., Cerrato, F., Ortega, H., Teruel, J. L., Lucas, M. F., Gómez-Coronado, D., Ortuño, J., & Lasunción, M. A. (2006). Concentrated red grape juice exerts antioxidant, hypolipidemic, and antiinflammatory effects in both hemodialysis patients and healthy subjects. *The American Journal of Clinical Nutrition*, 84(1), 252-262. http://dx.doi.org/10.1093/ajcn/84.1.252. PMid:16825703.

Egert, S., Bosy-Westphal, A., Seiberl, J., Kürbitz, C., Settler, U., Plachta-Danielzik, S., Wagner, A. E., Frank, J., Schrezenmeir, J., Rimbach, G., Wolffram, S., & Müller, M. J. (2009). Quercetin reduces systolic blood pressure and plasma oxidised low-density lipoprotein concentrations in overweight subjects with a high-cardiovascular disease risk phenotype: a double-blinded, placebo-controlled cross-over study. *The British Journal of Nutrition*, 102(7), 1065-1074. http://dx.doi.org/10.1017/S0007114509359127. PMid:19402938.

Huang, S., Ding, D., Chen, S., Dong, C., Ye, X., Yuan, Y., Feng, Y., You, N., Xu, J., Miao, H., You, Q., Lu, X., & Lu, Y. (2017). Resveratrol protects podocytes against apoptosis via stimulation of autophagy in a mouse model of diabetic nephropathy. *Scientific Reports*, 7(1), 45692. http://dx.doi.org/10.1038/srep45692. PMid:28374806.

Kim, K. H., & Lee, M. S. (2014). Autophagy: a key player in cellular and body metabolism. *Nature Reviews. Endocrinology*, 10(6), 322-337. http://dx.doi.org/10.1038/nrendo.2014.35. PMid:24663220.

Knekt, P., Kumpulainen, J., Järvinen, R., Rissanen, H., Heliövaara, M., Reunanen, A., Hakulinen, T., & Aromaa, A. (2002). Flavonoid intake and risk of chronic diseases. *The American Journal of Clinical Nutrition*, 76(3), 560-568. http://dx.doi.org/10.1093/ajcn/76.3.560. PMid:12198000.

Koch, E. A. T., Nakhoul, R., Nakhoul, F., & Nakhoul, N. (2020). Autophagy in diabetic nephropathy: a review. *International Urology and Nephrology*, 52(9), 1705-1712. http://dx.doi.org/10.1007/s11255-020-02545-4. PMid:32661628.

Li, S., Zhang, H., Du, Z., Li, C., An, M., Zong, Z., Liu, B., & Wang, H. (2016). Induction of epithelial-mesenchymal transition (EMT) by Beclin 1 knockdown via posttranscriptional upregulation of ZEB1 in thyroid cancer cells. *Oncotarget*, 7(43), 70364-70377. http://dx.doi.org/10.18632/oncotarget.12217. PMid:27683118.

Lin, R., Piao, M., Song, Y., & Liu, C. (2020). Quercetin suppresses AOM/DSS-Induced colon carcinogenesis through its anti-inflammation effects in mice. *Journal of Immunology Research*, 2020, 9242601. http://dx.doi.org/10.1155/2020/9242601. PMid:32537472.

Liu, X., Sun, N., Mo, N., Lu, S., Song, E., Ren, C., & Li, Z. (2019). Quercetin inhibits kidney fibrosis and the epithelial to mesenchymal transition of the renal tubular system involving suppression of the Sonic Hedgehog signaling pathway. *Food & Function*, 10(6), 3782-3797. http://dx.doi.org/10.1039/C9FO00373H. PMid:31180394.

Loeffler, I., & Wolf, G. (2015). Epithelial-to-mesenchymal transition in diabetic nephropathy: fact or fiction? *Cells*, 4(4), 631-652. http://dx.doi.org/10.3390/cells4040631. PMid:26473930.

Lu, Q., Ji, X., Zhou, Y., Yao, X., Liu, Y., Zhang, F., & Yin, X. (2015). Quercetin inhibits the mTORC1/p70S6K signaling-mediated renal tubular epithelial-mesenchymal transition and renal fibrosis in diabetic nephropathy. *Pharmacological Research*, 99, 237-247. http://dx.doi.org/10.1016/j.phrs.2015.06.006. PMid:26151815.

Luis-Rodríguez, D., Martínez-Castelao, A., Górriz, J. L., De-Álvaro, F., & Navarro-González, J. F. (2012). Pathophysiological role and therapeutic implications of inflammation in diabetic nephropathy. *World Journal of Diabetes*, 3(1), 7-18. http://dx.doi.org/10.4239/wjd.v3.i1.7. PMid:22253941.

Ma, L., Fu, R., Duan, Z., Lu, J., Gao, J., Tian, L., Lv, Z., Chen, Z., Han, J., Jia, L., & Wang, L. (2016). Sirt1 is essential for resveratrol enhancement of hypoxia-induced autophagy in the type 2 diabetic nephropathy rat. *Pathology, Research and Practice*, 212(4), 310-318. http://dx.doi.org/10.1016/j.prp.2016.02.001. PMid:26872534.

Recouvreux, M. V., Moldenhauer, M. R., Galenkamp, K. M. O., Jung, M., James, B., Zhang, Y., Lowy, A., Bagchi, A., & Commisso, C. (2020). Glutamine depletion regulates slug to promote EMT and metastasis in pancreatic cancer. *The Journal of Experimental Medicine*, 217(9), e20200388. http://dx.doi.org/10.1084/jem.20200388. PMid:32510550.

Rohatgi, R. A., & Shaw, L. M. (2016). An autophagy-independent function for Beclin 1 in cancer. *Molecular & Cellular Oncology*, 3(1), e1030539. http://dx.doi.org/10.1080/23723556.2015.1030539. PMid:26998512.

Tang, J., Diao, P., Shu, X., Li, L., & Xiong, L. (2019). Quercetin and quercitrin attenuates the inflammatory response and oxidative stress in LPS-Induced RAW264.7 cells: in vitro assessment and a theoretical model. *BioMed Research International*, 2019, 7039802. http://dx.doi.org/10.1155/2019/7039802. PMid:31781635.

Vindis, C. (2015). Autophagy: an emerging therapeutic target in vascular diseases. *British Journal of Pharmacology*, 172(9), 2167-2178. http://dx.doi.org/10.1111/bph.13052. PMid:25537552.

Wong, S. K., Chin, K.-Y., & Ima-Nirwana, S. (2020). Quercetin as an agent for protecting the bone: a review of the current evidence. *International Journal of Molecular Sciences*, 21(17), 6448. http://dx.doi.org/10.3390/ijms21176448. PMid:32899435.

Wu, W., Zhang, M., Liu, Q., Xue, L., Li, Y., & Ou, S. (2015). Piwil 2 gene transfection changes the autophagy status in a rat model of diabetic nephropathy. *International Journal of Clinical and Experimental Pathology*, 8(9), 10734-10742. PMid:26617784.

Xu, Y., Liu, L., Xin, W., Zhao, X., Chen, L., Zhen, J., & Wan, Q. (2015). The renoprotective role of autophagy activation in proximal tubular epithelial cells in diabetic nephropathy. *Journal of Diabetes and Its Complications*, 29(8), 976-983. http://dx.doi.org/10.1016/j.jdiacomp.2015.07.021. PMid:26297217.

Xu, Y., Ouyang, C., Lyu, D., Lin, Z., Zheng, W., Xiao, F., Xu, Z., & Ding, L. (2020). Diabetic nephropathy execrates epithelial-to-mesenchymal transition (EMT) via miR-2467-3p/Twist1 pathway. *Biomedicine and Pharmacotherapy*, 125, 109920. http://dx.doi.org/10.1016/j.biopha.2020.109920. PMid:32050151.